

## Miami Redblade III: A GPS-aided Autonomous Lawnmower

G. Newstadt, K. Green, D. Anderson, M. Lang, Y. Morton, and J. McCollum  
*Miami University, Oxford, Ohio.*

### Abstract

This paper describes the technical aspects of the Redblade III, Miami University's third generation autonomous lawnmower. The Redblade III was created for entrance in the Institute of Navigation's 4th Annual Autonomous Lawnmower Competition by a team of undergraduate students majoring in electrical, computer, and mechanical engineering at Miami University. This paper details the five major subsystems of the lawnmower, including (1) the sensing system, (2) the control system, (3) the mechanical chassis system, (4) the safety system, and (5) the base monitoring and testing system. The paper discusses each aforementioned system in detail, along with providing cost analysis and conclusions.

**Keywords:** Autonomous vehicle, GPS, DGPS

### 1. Background Introduction

The Redblade III is the third-generation autonomous lawnmower designed at Miami University of Ohio for entrance in the Institute of Navigation's (ION) 4th Annual Autonomous Lawnmower Competition. Previous generations of the Redblade were entered in the ION competitions in 2004 [1] and 2005 [2]. Moreover, the fourth generation Redblade was recently entered in the 2008 competition, though it will not be discussed here.

The ION Autonomous Lawnmower Competition consisted of the design and testing of autonomous vehicles for mowing a lawn of known shape. The lawnmowers were required to have no remote controls outside of a wireless remote emergency stop capability. Moreover, no local installations (buried wires, poles) were allowed, except for a Global Positioning System (GPS) local base station. The competition's complexity has increased over the years by changing the shape of the

field (rectangular to L-shaped) and including moving obstacles, among other changes.

The first generation Redblade [1] incorporated differential GPS (DGPS) and Hall-effect sensors for precise positioning, and a two level control system for path planning and error correction. However, the Redblade I base mower was modified from a commercial unit, and was both bulky and difficult to modify. The Redblade II [2] created a custom mechanical chassis to overcome these difficulties. Moreover, it replaced the Hall-effect sensors with much more effective and accurate optical encoders through the RobotEQ AX2550 system (see following sections for further description).

Lastly, the Redblade III was designed to improve on the previous generations in two important ways: (1) increased robustness through a redesigned DGPS system and the introduction of a digital compass; and (2) the ability to sense and react to moving obstacles. The rest of this paper outlines the design of the Redblade III in much greater detail, a relevant cost analysis, and conclusions.

### 2. Systems Overview

The design of the Miami Redblade III, is subdivided into five main systems: the sensing system, the control system, the monitoring and testing system, the safety system, and the base mower mechanical chassis system. Fig. 1 shows a flow diagram representing the relationships between these five bus-systems. Fig. 2 displays a picture of the final physical implementation of the lawnmower.

As stated above, Redblade III is an extension of previous autonomous lawnmowers at Miami University and it draws much of its design from its predecessors.

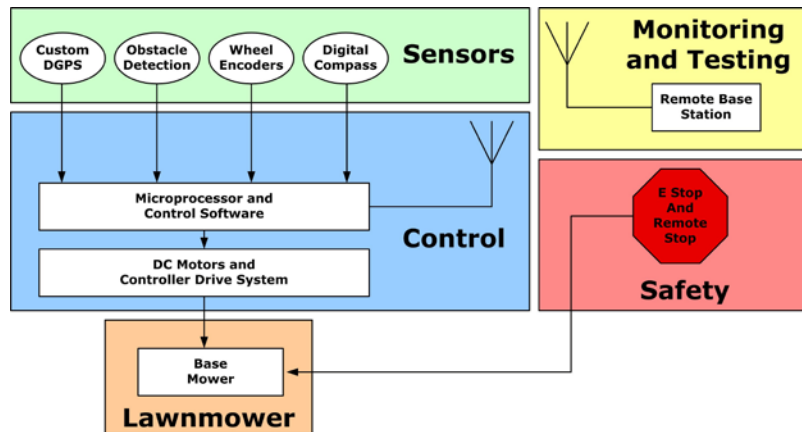


Fig. 1 Systems overview flow diagram

The current implementation employs the same mechanical chassis system and safety system of the Miami Redblade II. However, the current lawnmower has been upgraded with a modified DGPS system, new wheel encoders, and a more advanced control system. Furthermore, acoustic sensors and a laser ranging system have been added in order to supply obstacle detection capabilities.



Fig. 2 Physical implementation of the Redblade III

### 3. Sensing System

The sensing system is comprised of three parts: a differential global positioning system receiver (DGPS), an electronic compass, wheel encoders, and acoustic sensors. The DGPS system consists of two NovAtel Superstar II GPS receivers [3], a wireless radio link, and custom carrier phase-based precision RTK position algorithms developed at Miami by the team. The Honeywell HRM3200 electronic compass [4] provides heading information during turning as well as ensuring the mower does not start to drift from its expected heading in between waypoints. The wheel encoders use a US Digital E7MS quadrature optical encoder [5] in order to determine the position and velocity of the

lawnmower between DGPS solution updates. Each of these sensors will be discussed in greater detail in the following sections.

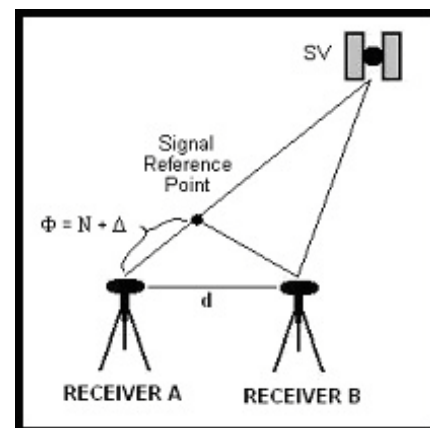


Fig. 3 Carrier phase integer ambiguity resolution

#### Custom DGPS

Navigation with GPS has become ubiquitous with the advent of personal GPS receivers in recent years. However, typical single frequency, civilian GPS receivers provide position accuracy only at the meter level [6]. The addition of another GPS receiver, on the other hand, allows the reduction of many correlated errors, including those due to the propagation through the ionosphere and troposphere, the satellite clock and orbit error, and the ephemeris error, provided that the baseline between the two receivers is not large. Our DGPS system is based on carrier phase measurements to provide accuracy at the centimeter level. Also, our system takes advantage of the fact that we initially know the exact relative positions of our receivers. This is done by precisely align the two receivers with a fixed distance between them. This allows our algorithms to quickly calculate the carrier phase integer ambiguities. Once these ambiguities have been

calculated, one of the receivers is allowed to roam freely, and the relative positions are calculated using an iterative linear minimization algorithm. Fig. 4 displays a schematic representing the integer ambiguity resolution that is used in our code. For a detailed explanation of how the DGPS system works and all of the mathematics that is involved, see Appendix A.

The DGPS operates updates with a rate of 1 Hz. Since the lawnmower's allowed maximum speed is 10km/hour which implies that it can move about 3 m in one second. Such distance can greatly impact the quality of mowing and may have consequences in safety. It is important that other systems be employed to locate the vehicle in between the times of the DGPS updates. The subsequent section describes the wheel encoder system that is used for this purpose.

### Wheel Encoders

The wheel encoders on Redblade III use US Digital E7MS quadrature optical encoders which are installed inside of the motors. Each encoder has two different signal channels which have phases that are 90 degrees apart. Each time the optical sensor detects a change, a pulse is sent to one of the signal channels, and a second pulse is sent 90 degrees offset from the first pulse. With this two channel configuration, detecting whether the wheel is moving forward or backwards becomes possible. Because the number of pulses there are per revolution of the wheel is known, dead-reckoning is used to compute the distance the mower has moved. This information is also applied to the encoders with a Proportional Integral Derivative (PID) control loop. In order to make both of the wheels turn at the exact same speed, an encoder module from RobotEQ [7] was purchased which was installed directly into the existing RobotEQ DC controller. The encoder module decodes the pulse train coming from the quadrature optical encoders and increments or decrements a counter register in the RobotEQ DC controller depending on if the wheel is going forward or in reverse.

This short-term dead-reckoning system not only fills the data gap between DGPS updates, it also provides redundant measurements to ensure the integrity of the DGPS. The DGPS is used to correct the errors that would accumulate if only wheel encoders were used to determine position.

### Digital Compass

The Honeywell HMR3200 digital compass uses magneto-resistive sensors to determine heading information. The HMR3200 is a two-axis compass that is used to compute the azimuth angle of the lawnmower. The compass supplies data at rate of up to 15 Hz. The compass data is used primarily to orient the lawnmower turning rotations, though it can also

serve to correct the path of the lawnmower if the heading diverges too much from the expected value.

### Obstacle Detection

Two sensors were considered for obstacle detection and avoidance. The first is a SICK LMS200 Laser Range Finder (see Fig. 8). The LMS200 uses a laser to detect the distance an object is away from the unit, providing 180 degree visibility about a vertical axis and a 30 meter range. Furthermore, objects can be detected at a centimeter level accuracy.

The second sensor is a parallax acoustic sensor which uses the properties of sound to detect the distance of an object from the sensor. The acoustic sensor only has a range of 3 meters and accuracy much less than the laser ranging system described above. On the other hand, it is considerably cheaper and may be sufficient for the obstacle avoidance that our lawnmower requires.

Due to the overwhelming precision and accuracy of the laser ranging sensor, we decided to use the SICK LIDAR. However, we found that this system has the tendency to be tricked into thinking an obstacle is there when no obstacle exists (which can occur when sunlight is directly inputted into the laser). Thus, future implementations may use acoustic sensors as redundant measurements.

## 4. Control System

The control algorithm is executed on a notebook computer that is mounted on the Redblade III. All of the various electronics, motor controllers, and sensors are connected to the computer using RS232 connections. The lawnmower incorporates a RobotEQ DC Motor Controller that is also controlled by the computer. The RobotEQ DC Motor Controller has a built-in PID control loop that enables the two separate motors to move concurrently and at the same speed. The wheel encoders are also connected directly to the RobotEQ, providing the fastest information to the PID controller.

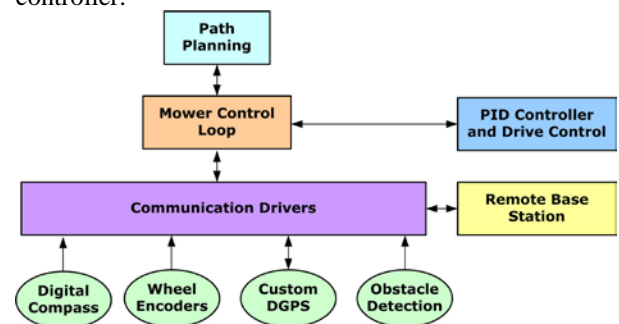


Fig. 4 Control systems integration flow diagram

### Overview and system integration

The control software consists of four major components: (1) High-level path planning and control; (2) a control loop to determine and correct the current lawnmower position with regard to the path-planning, sensor inputs, and obstacle detection; (3) low-level communication interfacing between the control loop and the sensors, the actuators, and the remote base station; and (4) a PID controller to direct the lawnmower while it is moving. Fig. 4 shows a flow diagram of the integration of these systems.

The control software provides the option to control the path planning through the remote base station for testing and monitoring purposes. Furthermore, several exterior utilities were created to complete such tasks as forecasting satellite availability.

All of the software is written in Java. An object-oriented approach was implemented to provide the most flexibility for the project. Extensive class libraries were created for the systems described above, and a detailed model description of these libraries is available upon request.

### Control Algorithm

The control algorithm is shown as a flow diagram in Fig. 5. The algorithm is composed of four main

components: (1) System initialization; (2) path planning and control, including the ability to dynamically change the planned path based on obstacle detection and/or discovered errors in the path travelled by the lawnmower; (3) orientation change; (4) position change; and (5) obstacle detection.

It is important to note several things about the control algorithm. First, while the lawnmower is moving, all position estimates are computed using the information supplied by the wheel encoders. The compass will provide heading information to control the turning angles at the desired location. Furthermore, the PID controller uses the wheel encoder data to dynamically control the drive system during this time.

Second, the DGPS system is used to calculate precise locations once the lawnmower has come to a stop, which occurs when the lawnmower has reached its desired location or has encountered an obstacle. However, the DGPS calculated position may not line up exactly with the desired location of path planning, and the detected obstacle may make it impossible to travel to the correct endpoint. At this point, the path planning's dynamic capabilities allow the lawnmower to update its next desired position based on the decision to correct any error in the path already travelled or to avoid an obstacle.

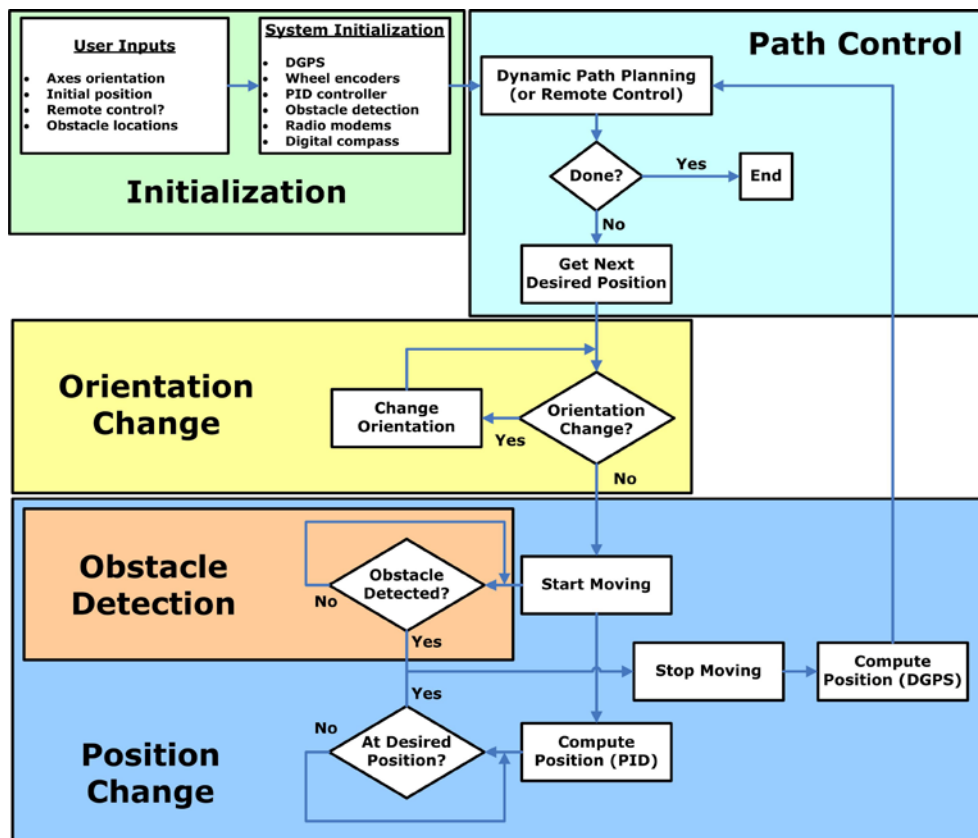


Fig. 5 Control algorithm flow diagram

Third, while testing has given us confidence that our systems work as designed, we have built in robustness checks based on the redundant data given by our multiple sensors. Furthermore, the DGPS system has the ability to re-initialize itself if it has determined that it is no longer functioning in a valid state. This algorithm is described in the subsequent section.

### DGPS Control

The DGPS is normally a well-functioning system. However, occasionally the system will cease to operate in a valid state, such as when it ceases to track a minimum of four satellites. This can occur if the signals from the tracked satellites are blocked in some fashion. For this reason, it is important that mission planning be done before the lawnmower is actually operated, and the aforementioned satellite availability forecasting software was designed for exactly this purpose.

Nevertheless, with the possibility of invalid position data being generated by the DGPS, an algorithm to re-initialize the system was developed for the sake of robustness and reliability. The flow diagram of this algorithm is shown in Fig. 6. It is important to note

that the DGPS determines whether it is in a valid state within the software package. Considerations for validity include the number of tracked satellites, limits on the calculated positions with respect to previously calculated positions (the lawnmower can only move so far in a set period of time), and consensus with the redundant data given by other sensors. Additionally, when being re-initialized, the DGPS has to assume that the positions given by the other sensors are completely accurate. While this may introduce some error to the system as a whole, the DGPS is integral to a fully-functioning autonomous lawnmower, so the error is tolerated.

### Path Control Algorithm

The path control is divided into two major components: (1) path planning; and (2) decision making based on external sensors. This algorithm is shown in a flow diagram in Fig. 7. The path planning is computed initially before the lawnmower begins moving and outputs a set of waypoints for the lawnmower to follow. At each waypoint, the lawnmower updates its position through the DGPS, changes its orientation, checks its heading, or does some combination of these actions.

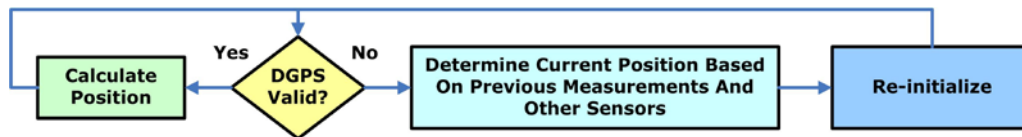


Fig. 6 DGPS control flow diagram

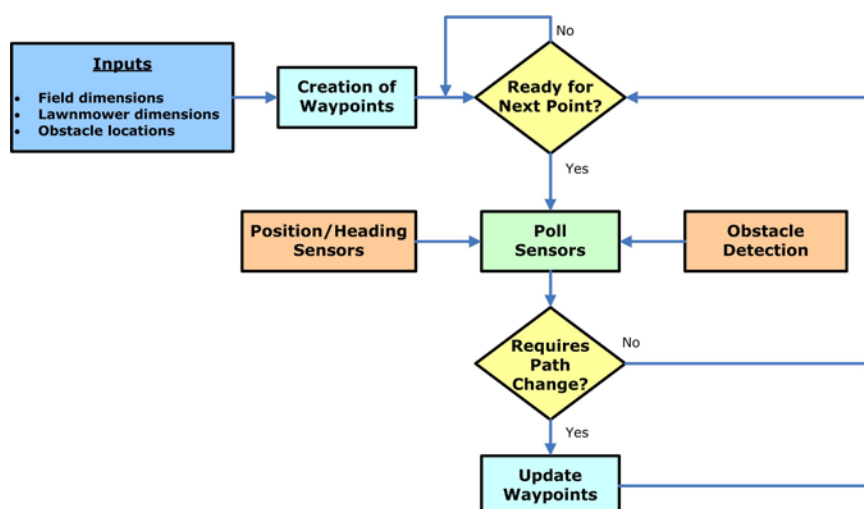


Fig. 7 Path control flow diagram

The path planning is computed based on a set of initial parameters. These parameters include the field's dimensions (assuming a rectangular geometry), the obstacle size and locations, and the lawnmower's dimensions (such as width, length, and cutting blade length). The waypoints are generated in such a way to insure that the lawnmower never leaves the boundary while moving or turning. Furthermore, the turns are constructed in such a way to never place any part of the mower outside of the boundary. Additionally, static obstacle avoidance is pre-computed to make arbitrary radial turns that will allow for smooth motion around each obstacle. These turns are done to ensure mowing in a safe zone as well as to be aesthetically pleasing. Fig. 8 shows a graphical output of the initial computed waypoints given two obstacles with different sizes.

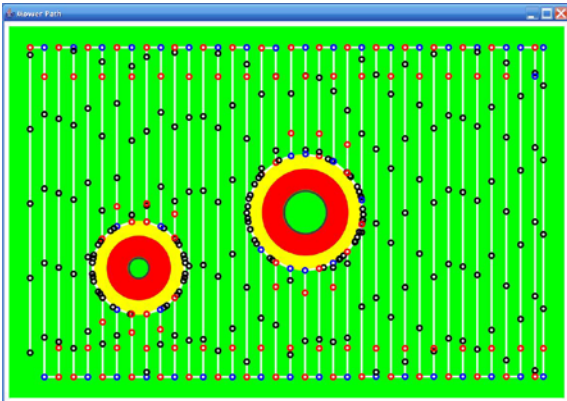


Fig. 8 Waypoint configuration for two obstacles with different sizes

The path control also incorporates decision making based on external sensors. This includes updating the path waypoints when an obstacle is encountered or when position sensors (location and heading) indicate that the lawnmower is off-target past a certain threshold.

## 5. Drive and Power System

The control system described in the previous section is critical to the functioning of the Redblade III, but without the drive and power system, it would be completely useless. The Redblade III incorporates a drive system with two Power Chair (NPC) model T64 24-Volt DC motors and a hybrid power system consisting of rechargeable batteries and a gas engine. The individual drive and power systems are described in the following sections.

### Drive system

The drive system consists of two Power Chair (NPC) model T64 24-Volt DC motors. The DC motors are voltage-controlled with a low RPM-torque of approximately 300 in-lbs. Furthermore, the motors are

equipped with a 20:1 gear ratio to give suitable RPM ranges for operation. The DC motor and wheel couplings are pictured in Fig. 9.



Fig. 9 DC motor and wheel coupling implementation

### Power system

The power system incorporates both rechargeable batteries and a gas engine. The Redblade III employs two Power-Sonic sealed lead acid (SLA) batteries. The low-cycle batteries output 12 Volts and 7 amp-hours, and are connected in series to provide 24 V to the DC motors and the various on-board electronics. The batteries are rechargeable through ordinary AC power outlets while the lawnmower is stationary. Currently, our design does not incorporate any way to charge the batteries while the lawnmower is operating, though future work includes integrating an alternator for this purpose.

The Redblade III also utilizes a 5.5 horsepower gas engine in order to provide sufficient rotational energy to the cutting blade. Fig. 10 highlights the power system on board of the lawnmower.



Fig. 10 Power system on the Redblade III

### Wiring diagram

The wiring diagram of the drive and power system is shown in Fig. 11.

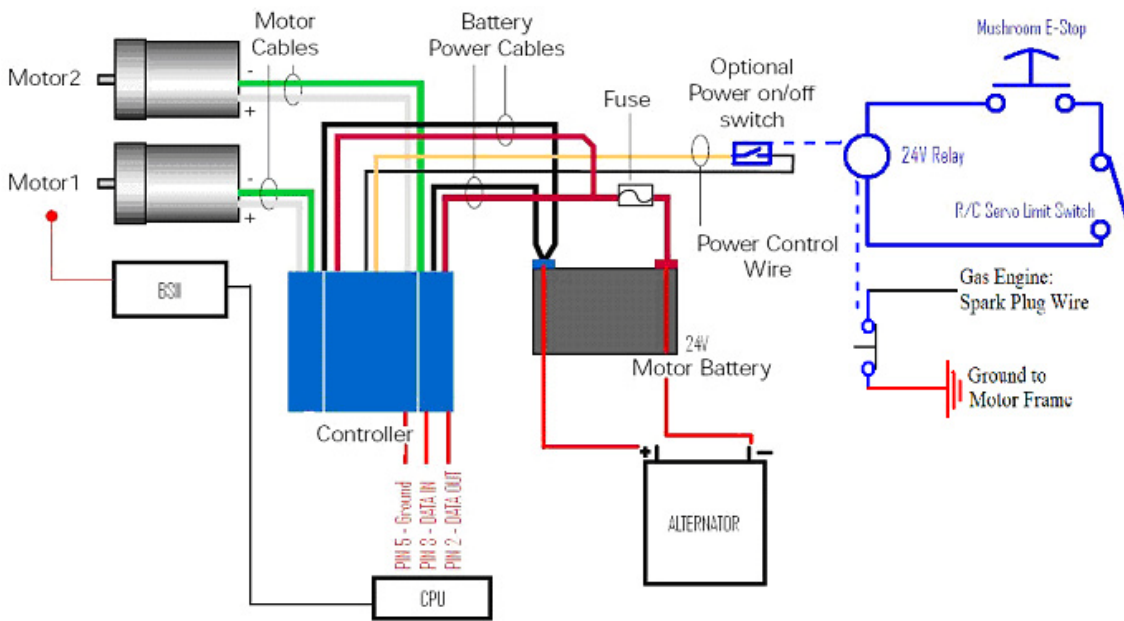


Fig. 11. Wiring diagram

## 6. Mechanical Chassis System

The mechanical chassis system was designed to optimally integrate all of the previously discussed systems in a physical manner. The lawnmower is lightweight, yet robust. It is framed with angle iron, and the mounting surfaces are shielded with high strength steel sheeting with plywood covering the steel. Furthermore, a shelving system was incorporated to offer the maximum flexibility to our layout and construction.

The top shelf (see Fig. 12) houses the gas engine. The bottom shelf (see Fig. 13) holds most of the electronics, including the notebook computer, the batteries, the RobotEQ controller, the GPS receiver (and radio modem), and the power circuitry. Specialized mounts were created for the laser ranging system, the safety switch, the digital compass, and the GPS antenna (see Fig. 14).



Fig. 12 Top shelf (gas engine)

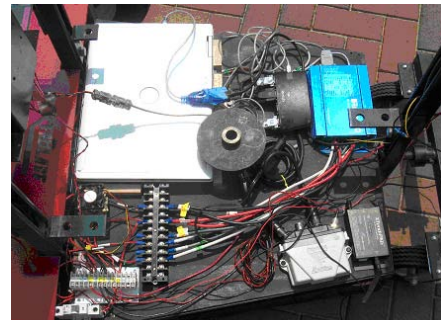


Fig. 13 Bottom shelf (electronics, batteries, etc.)



Fig. 14 Specialized mounts: laser ranging system (top left), safety switch (top right), digital compass (bottom left), and GPS antenna (bottom right).

Two 6" pneumatic caster wheels with 4"x4" mounting plates were custom-designed for the lawnmower. The pneumatic nature assists in the handling of rocky and unstable terrains, such as may be the case with mowing field. Additionally, the casters were mounted to a shaft in

the front to allow the caster assembly to pivot vertically. This allows either front wheel to encounter a ditch or imperfection in the field without causing the rear wheels to lift up. This design ensures that the base of the lawnmower remains at a relatively constant height and gives the lawnmower the ability to always propel itself out of a hole. Fig. 15 shows the implementation of the caster wheels. The rear wheels drive the vehicle with diameters of 16.5".



Fig. 15 Caster wheels implementation

A unique shaft coupling design was created to link the gas engine to the alternator shaft and the cutting blade. This provides the ability to disengage the blade while still running the alternator, which was very desirable for testing purposes. Fig. 16 displays the shaft coupling mechanism.

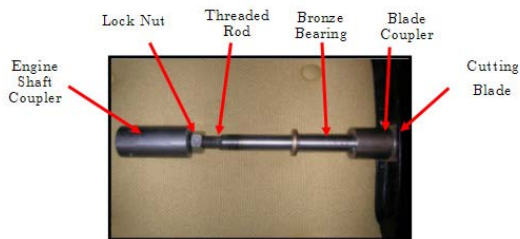


Fig. 16 Shaft coupling mechanism

## 7. Safety System

With a large vehicle attached with a cutting blade that could cause considerable damage, it is of utmost importance that a reliable safety system be implemented. For the Redblade III, an on-board emergency stop and a remote-controlled emergency stop provided for this purpose. The emergency stop system allows the user to stop all motion on the lawnmower (e.g., the DC motors and the gas engine). Fig. 17 shows the emergency stop circuit. A 24 V relay controls this circuit, which can be broken by a normally closed emergency stop button that is easily accessible from the rear of the lawnmower. A normally open limit switch also can cause the power

circuit to be broken. The limit switch is held closed by an RC servo that is kept in tension via a spring mounted to the control panel. Thus, the user can easily open the limit switch (causing the power circuit to be broken) by releasing the RC control trigger. Furthermore, since the limit switch is normally open, if the RC controller is dropped or loses power, the emergency stop will be activated, creating a desired fail-safe mode of operation.

The RobotEQ motor controller has an optional on/off switch controlled by two wires connected through a normally closed port controlled by the 24 V relay. Thus, if the relay loses power (i.e., the power circuit has been broken) then the RobotEQ will also lose power.

Stopping the motion of the gas engine requires that the spark plug be grounded to the motor frame. The 24 V relay is therefore connected in series with the spark plug, causing the gas engine to lose power when the 24 V relay loses power.

## 8. Base Station Monitoring and Testing Station

A base station for remote monitoring and testing was developed to accompany the Redblade III. The base station is comprised of a PC with wireless communication capabilities, a custom-designed user interface, remote control, and data logging programs. The remote monitoring and testing software was written in Java.

## 9. Conclusions

The Redblade III is Miami University's third generation autonomous lawnmower. It has incorporated many changes, including the addition of robust custom DGPS, advanced control algorithms, wheel encoder sensors, obstacle detection capabilities, and an updated mechanical chassis.

Further improvements could include replacing the onboard notebook computer with a dedicated microprocessor, as well as using an inertial momentum unit (IMU) to replace the noisier digital compass. Lastly, the use of multiple sensors may lead us to use more advanced, adaptive processing for control. At the very least, we could employ Kalman or particle filtering to provide optimal (or near-optimal) control.

Overall, the Redblade III is much more robust and reliable than in previous generations, though it still offers much of the same flexibility and ability for improvement that was seen in the Redblade II. Although there is still room for significant improvement, we are pleased with the progress of the lawnmower and believe that the autonomous lawnmowers may be an achievable consumer goal in the near future.

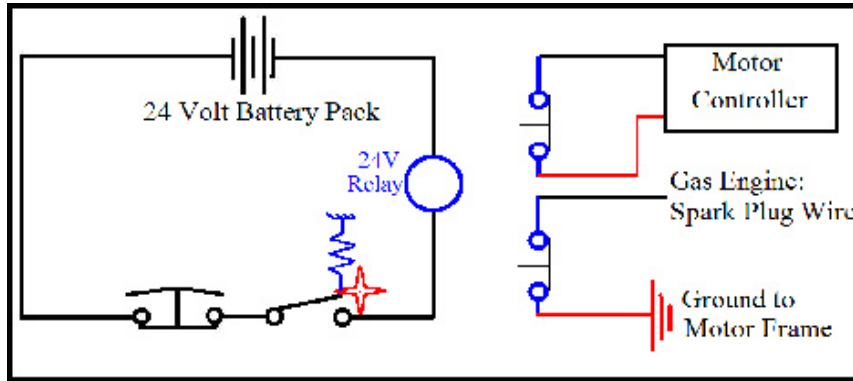


Fig. 17 Emergency stop circuits for the 24 V relay (left), RobotEQ controller (top right), and gas engine (bottom right)

### Appendix: DGPS algorithm description

The integer ambiguities associated with the carrier phase are integral to the precise positioning of the user. This methodology of ambiguity resolution takes into account the fact that we originally know the *exact* distance between our two receivers at the initial time. Fig. 3 shows the two-dimensional arrangement of a satellite and our two receivers. When we know the distance between the USER and the REFERENCE (12 inches) and the related pseudoranges, the ambiguity,  $N$ , is easily solved through some basic geometry.

However, due to errors in the atmosphere (ionospheric, tropospheric delays) and satellite clock errors, we would not expect reliable ambiguity calculations by using just one satellite. Instead, we use double-differencing techniques to remove these correlated errors. The formula we use to calculate the ambiguities is given by:

$$N_{ur}^{i,1} = \frac{R_{ur}^{i,1}}{\lambda} - \phi_{ur}^{i,1}$$

where  $R$  refers to the range in meters, and  $\phi$  is the carrier phase in radians. Also, the subscripts refer to the USER ( $u$ ) and the REFERENCE ( $r$ ) receivers, the superscripts refer to the BASE satellite (1) and the other satellites ( $i$ ), and the notation in the formula is defined as:

$$(*)_{ur}^{i,1} = \left( \left( (*)_u^i - (*)_u^1 \right) - \left( (*)_r^i - (*)_r^1 \right) \right)$$

Furthermore, since we already know the original orientation of our USER and REFERENCE receivers, and the carrier phases are provided by the receivers themselves, we only have 1 equation with 1 unknown, and our ambiguity resolution is complete. However, it is important not only to resolve the ambiguities, but to also to consistently calculate the *same* ambiguities over a period of time. Therefore, the code requires that each

ambiguity must be calculated the same way 20 times in a row before allowing the USER to roam.

The range equation with regard to the carrier phase is given by

$$\lambda \phi_r^i = \lambda \hat{\phi}_r^i + C^i + I_r^i + T_r^i$$

where the latter terms refer to the satellite clock error, ionospheric delay, and tropospheric delay, respectively. However, from equation (1), we know we can solve for the USER position by knowing the relationship:

$$R_u^{i,1} - R_r^{i,1} = R_{ur}^{i,1} = \lambda \phi_{ur}^{i,1} + \lambda N_{ur}^{i,1}$$

Furthermore, if we use a first-order Taylor expansion, and expand it to three dimensions ( $xyz$ ), we will get the matrix equation:

$$A_j^i * D = L^i$$

for  $i = 2, \dots, N$  and  $j = 1, 2, 3$  and

$$A_1^i = \frac{X^i - X_u(0)}{R_u^i(0)} - \frac{X^1 - X_u(0)}{R_u^1(0)}$$

$$A_2^i = \frac{Y^i - Y_u(0)}{R_u^i(0)} - \frac{Y^1 - Y_u(0)}{R_u^1(0)}$$

$$A_3^i = \frac{Z^i - Z_u(0)}{R_u^i(0)} - \frac{Z^1 - Z_u(0)}{R_u^1(0)}$$

$$D = \begin{bmatrix} \Delta X \\ \Delta Y \\ \Delta Z \end{bmatrix}$$

$$L^i = \lambda \phi_{ur}^{i,1} + \lambda N_{ur}^{i,1} + (R_r^i(0) - R_r^1(0)) - (R_u^i(0) - R_u^1(0))$$

where variables with subscripts refer to measurements from the receivers, while variables with superscripts refer to measurements from the satellites. Also, this system of equations can be solved with a least-squares solution to get:

$$D = (A'Q^{-1}A)^{-1} (A'Q^{-1})L$$

where  $Q$  is the sample covariance matrix. The user position is then given by:

$$R_u = \begin{bmatrix} X_u \\ Y_u \\ Z_u \end{bmatrix} = R_u(0) - D = \begin{bmatrix} X_u(0) - \Delta X \\ Y_u(0) - \Delta Y \\ Z_u(0) - \Delta Z \end{bmatrix}$$

Lastly, this process of calculating the position is done iteratively until the delta matrix,  $D$ , becomes approximately zero (less than  $1e-9$ ).

## References

- [1] McNally B., Stutzman M., Koranda C., Mantz C., Macsek J., Miller S., Walker A., Morton J., Campbell S., Leonard J (2004) *The Miami Redblade: Technical Report*, Institute of Navigation Autonomous Lawnmower Competition.
- [2] French M., Russler J., Smith J., Smith L., Walters T., Morton J., Campbell S., Leonard J. (2005) *The Miami Redblade II: Technical Report*, Institute of Navigation Autonomous Lawnmower Competition.
- [3] NovAtel Superstar II GPS receiver circuit board, <http://www.novatel.com/products/superstar.htm>.
- [4] Honeywell HMR3200/HMR3300 digital compass, <http://www.ssec.honeywell.com/magnetic/datasheets/hmr32003300.pdf>.
- [5] Metal optical kit encoder – e7m, <http://www.usdigital.com/products/e7m/>.
- [6] Misra P. and Enge P. (2005) *Global Positioning Systems: Signals, Measurement, and Performance*. Ganga-Jamuna Press: 147-282.
- [7] Roboteq: Ax2550, <http://www.roboteq.com/ax2550-folder.html>.